

# Six New Metal–Organic Frameworks Based on Polycarboxylate Acids and V-shaped Imidazole-Based Synthon: Syntheses, Crystal Structures, and Properties

Jinsong Hu,<sup>†</sup> Liangfang Huang,<sup>†</sup> Xiaoqiang Yao,<sup>†</sup> Ling Qin,<sup>†</sup> Yizhi Li,<sup>†</sup> Zijian Guo,<sup>†</sup> Hegen Zheng,<sup>\*,†,‡</sup> and Ziling Xue<sup>\*,§</sup>

<sup>†</sup>State Key Laboratory of Coordination Chemistry, School of Chemistry and Chemical Engineering, Nanjing National Laboratory of Microstructures, Nanjing University, Nanjing 210093, People's Republic of China

<sup>‡</sup>State Key Laboratory of Structural Chemistry, Fujian Institute of Research on the Structure of Matter, Chinese Academy of Sciences, Fuzhou 350002, People's Republic of China

<sup>§</sup>Department of Chemistry, The University of Tennessee, Knoxville, Tennessee 37996-1600, United States

 Supporting Information

**ABSTRACT:** Solvothermal reactions of 4,4'-bis(imidazol-1-yl)diphenyl ether (BIDPE) with deprotonated 5-hydroxy-isophthalic acid (5-OH-H<sub>2</sub>bdc), and benzene-1,3,5-tricarboxylic acid (H<sub>3</sub>btc) in the presence of cadmium(II), zinc(II), cobalt(II), nickel(II), and manganese(II) salts in H<sub>2</sub>O or H<sub>2</sub>O/DMF produced six new complexes, namely, [Cd(BIDPE)(5-OH-bdc)·H<sub>2</sub>O]<sub>n</sub> (1), [Co(BIDPE)(5-OH-bdc)·H<sub>2</sub>O]<sub>n</sub> (2), [Zn<sub>3</sub>(BIDPE)<sub>3</sub>(5-OH-bdc)<sub>3</sub>·4H<sub>2</sub>O]<sub>n</sub> (3), [Ni(BIDPE)<sub>2</sub>(5-OH-bdc)(H<sub>2</sub>O)·3H<sub>2</sub>O]<sub>n</sub> (4), {[Mn<sub>2</sub>(BIDPE)<sub>2</sub>(5-OH-bdc)<sub>2</sub>]<sub>n</sub> (5), and [Ni(BIDPE)<sub>2</sub>(Hbtc)(H<sub>2</sub>O)]<sub>n</sub> (6). These complexes were characterized by elemental analysis, IR spectroscopy, and X-ray single-crystal diffraction. Compounds 1 and 2 reveal the same two-dimensional (2D) sheets with a 32-membered [(Cd/Co)<sub>2</sub>(BIDPE)<sub>2</sub>] metallocyclic ring constructed from BIDPE and 5-OH-H<sub>2</sub>bdc with Cd or Co salts. For compound 3, six identical 2D sheets are polycatenated in parallel to form a rare 2D → 2D framework; it displays ferroelectric behavior with a remnant electric polarization (*P<sub>r</sub>*) of 0.033 μC/cm<sup>2</sup> and an electric coercive field (*E<sub>c</sub>*) of 11.15 kV/cm. In compounds 4 and 6, only one carboxyl group coordinated to the Ni atom from 5-OH-H<sub>2</sub>bdc or H<sub>3</sub>btc. Compound 5 exists as binuclear Mn clusters, which are linked by BIDPE and 5-OH-H<sub>2</sub>bdc to generate a 2D sheet and displays weak antiferromagnetic character. In addition, the thermal stabilities and photochemical properties of these new complexes have been studied.

## INTRODUCTION

The designed construction of metal–organic frameworks (MOFs) from various molecular building blocks connected by coordination bond, supramolecular contacts, has been of intense interest, because of their intriguing aesthetic structures and topological features,<sup>1</sup> as well as their promising applications in photochemistry areas,<sup>2</sup> molecular magnetism,<sup>3</sup> heterogeneous catalysis,<sup>4</sup> and molecular sorption.<sup>5</sup> However, it is still a great challenge to rationally design and construct the desired compounds. Many factors, such as organic ligands,<sup>6</sup> solvent system,<sup>7</sup> metal ions,<sup>8</sup> and counterions,<sup>9</sup> are found to greatly influence the structures, rendering it difficult to predict the construction of molecular architectures. Therefore, systematic studies of diversified conditions leading to different structures in the formation of coordination polymers are important and of intense interest. Recently, a large number of mixed-ligand MOFs have been reported,<sup>10</sup> revealing that the combination of different ligands can result in greater tunability of structural frameworks than single ligands. Therefore, mixed ligands are a good choice for the construction of new polymeric structures.

Several N-donor ligands have been widely employed to construct coordination polymers with fascinating architectures and interesting properties.<sup>11</sup> Among the N-donor ligands, multidentate ligands with imidazole groups have attracted great interest.

Excellent coordination ability and free rotation of the imidazole ring in multidentate ligands meet the requirement of coordination geometries of metal ions in the assembly process. Until now, a great number of ingenious MOFs have been designed based on imidazole ligands.<sup>12</sup> We recently designed and synthesized 4,4'-bis(imidazol-1-yl) diphenyl ether (BIDPE, Scheme 1), which is a V-shaped imidazole ligand that can be regarded as a half-flexible ligand.<sup>13</sup> The H<sub>3</sub>btc and 5-OH-H<sub>2</sub>bdc are V-shaped or triangular ligands, which have some connects in structures. To test the ability of this ligand to give new architectures and topologies, we selected this ligand, 5-OH-H<sub>2</sub>bdc, H<sub>3</sub>btc (Scheme 1), and different bivalent metal salts to solvothermally synthesize six new coordination polymers with intriguing structures, namely, [Cd(BIDPE)(5-OH-bdc)·H<sub>2</sub>O]<sub>n</sub> (1), [Co(BIDPE)(5-OH-bdc)·H<sub>2</sub>O]<sub>n</sub> (2), [Zn<sub>3</sub>(BIDPE)<sub>3</sub>(5-OH-bdc)<sub>3</sub>·4H<sub>2</sub>O]<sub>n</sub> (3), [Ni(BIDPE)<sub>2</sub>(5-OH-bdc)(H<sub>2</sub>O)·3H<sub>2</sub>O]<sub>n</sub> (4), {[Mn<sub>2</sub>(BIDPE)<sub>2</sub>(5-OH-bdc)<sub>2</sub>]<sub>n</sub> (5), and [Ni(BIDPE)<sub>2</sub>(Hbtc)(H<sub>2</sub>O)]<sub>n</sub> (6). The new compounds have been characterized by elemental analysis, IR spectra, and X-ray crystallography. The crystal structures, topological analyses, and their thermal properties have been studied. In addition,

Received: November 2, 2010

Published: February 08, 2011

Scheme 1. The V-shaped Imidazole Ligand and Polycarboxylate Ligands

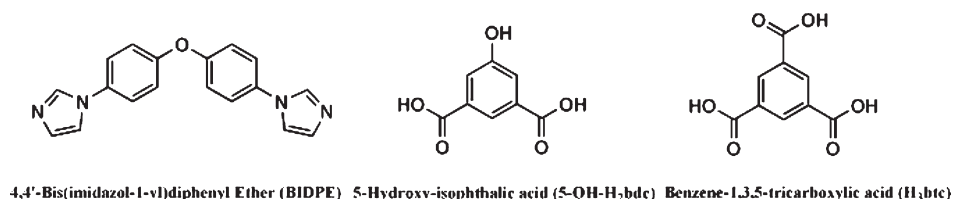


Table 1. Crystallographic Data for Complexes 1–6

	1	2	3	4	5	6
formula	C <sub>26</sub> H <sub>20</sub> O <sub>7</sub> N <sub>4</sub> Cd	C <sub>26</sub> H <sub>20</sub> O <sub>7</sub> N <sub>4</sub> Co	C <sub>78</sub> H <sub>62</sub> O <sub>22</sub> N <sub>12</sub> Zn <sub>3</sub>	C <sub>44</sub> H <sub>40</sub> O <sub>11</sub> N <sub>8</sub> Ni	C <sub>52</sub> H <sub>36</sub> O <sub>12</sub> N <sub>8</sub> Mn <sub>2</sub>	C <sub>45</sub> H <sub>36</sub> N <sub>8</sub> O <sub>9</sub> Ni
formula weight	612.87	559.39	1705.55	915.53	1074.66	891.50
crystal system	monoclinic	monoclinic	orthorhombic	monoclinic	monoclinic	monoclinic
space group	<i>P</i> 2 <sub>1</sub> / <i>n</i>	<i>P</i> 2 <sub>1</sub> / <i>n</i>	<i>Fdd</i> 2	<i>C</i> 2/ <i>c</i>	<i>P</i> 2 <sub>1</sub> / <i>c</i>	<i>P</i> 2 <sub>1</sub> / <i>c</i>
<i>a</i> (Å)	9.5126(10)	9.1980(10)	25.498(5)	26.548(2)	11.7405(10)	8.5856(12)
<i>b</i> (Å)	24.370(3)	24.288(3)	30.011(6)	10.1451(8)	19.0544(18)	18.375(3)
<i>c</i> (Å)	11.7544(12)	11.4782(12)	44.331(9)	30.495(2)	19.8722(18)	24.508(3)
$\alpha$ (deg)	90.00	90.00	90.00	90.00	90.00	90.00
$\beta$ (deg)	111.403(2)	108.909(2)	90.00	102.028(2)	97.039(2)	90.730(3)
$\gamma$ (deg)	90.00	90.00	90.00	90.00	90.00	90.00
<i>V</i> (Å <sup>3</sup> )	2537.0(5)	2425.9(5)	33923(12)	8033.0(11)	4412.1(7)	3866.1(10)
<i>Z</i>	4	4	16	100	4	4
<i>D</i> <sub>c</sub> (g cm <sup>−3</sup> )	1.605	1.532	1.329	1.514	1.618	1.828
$\mu$ (Mo) <i>K</i> $\alpha$ (mm <sup>−1</sup> )	0.914	0.763	0.917	0.559	0.653	0.575
<i>F</i> (000)	1232.0	1148	13920	3808	2200	2216
theta min–max (deg)	2.04, 25.00	1.68, 25.00	2.10, 25.00	2.29, 25.00	2.05, 25.00	1.66, 25.00
tot., uniq. data	12515	11966	41244	19378	21724	19051
<i>R</i> (int)	0.0317	0.0454	0.0523	0.0541	0.0572	0.0448
observed data [ <i>I</i> > 2 $\sigma$ ( <i>I</i> )] [ <i>I</i> > 2 $\sigma$ ( <i>I</i> )]	3948	3060	9877	4748	5620	5247
<i>R</i> <sub>1</sub> , <i>wR</i> <sub>2</sub> [ <i>I</i> > 2 $\sigma$ ( <i>I</i> )]	0.0450, 0.1290	0.0585, 0.1478	0.0749, 0.1824	0.0531, 0.1196	0.0481, 0.0858	0.0430, 0.0940
<i>S</i>	1.095	1.011	0.966	0.975	0.965	0.994
min. and max. Resdens (e Å <sup>−3</sup> )	−0.894, 1.138	−0.630, 0.972	−0.854, 1.944	−0.573, 0.655	−0.289, 0.361	−0.398, 0.436

photoluminescences, ferroelectric behavior, and magnetic character for complexes 1–6 are discussed in detail.

## EXPERIMENTAL SECTION

**Materials and Methods.** The reagents and solvents employed were commercially available and used as received. BIDPE was prepared by the literature methods.<sup>13</sup> IR absorption spectra of the complexes were recorded in the range of 400–4000 cm<sup>−1</sup> on a Nicolet (Impact 410) spectrometer with KBr pellets (5 mg of sample in 500 mg of KBr). C, H, and N analyses were carried out with a Perkin–Elmer 240C elemental analyzer. Powder X-ray diffraction (PXRD) measurements were performed on a Bruker D8 Advance X-ray diffractometer using Cu *K* $\alpha$  radiation ( $\lambda$  = 1.5418 Å), in which the X-ray tube was operated at 40 kV and 40 mA. Solid-state UV–vis diffuse reflectance spectra was obtained at room temperature using a Shimadzu UV-3600 double monochromator spectrophotometer, and BaSO<sub>4</sub> was used as a 100% reflectance standard for all materials. Luminescent spectra were recorded with a Shimadzu VF-320 X-ray fluorescence spectrophotometer at room temperature. The emission decay lifetimes were measured on an Edinburgh Instruments FLS920 fluorescence spectrometer. The electric hysteresis loops were recorded on a Ferroelectric Tester Precision Premier II made by Radiant Technologies, Inc. The as-synthesized samples were

characterized by thermogravimetric analysis (TGA) on a Perkin–Elmer thermogravimetric analyzer Pyris 1 TGA up to 1023 K, using a heating rate of 10 K min<sup>−1</sup> under N<sub>2</sub> atmosphere. Temperature-dependent magnetic susceptibility data were obtained on a MPMS XL-7 SQUID magnetometer under an applied field of 2000 Oe over the temperature range of 2–300 K.

**Syntheses of the Compounds.** [*Cd*(BIDPE)(5-OH-bdc)·H<sub>2</sub>O]<sub>*n*</sub> (**1**). A mixture of Cd(NO<sub>3</sub>)<sub>2</sub>·4H<sub>2</sub>O (30.1 mg, 0.1 mmol), 5-OH-H<sub>2</sub>bdc (18.2 mg, 0.1 mmol) and BIDPE (28.4 mg, 0.1 mmol) was dissolved in 9 mL of DMF/H<sub>2</sub>O (2:1, v/v). The final mixture was placed in a Parr Teflon-lined stainless steel vessel (15 mL) under autogenous pressure and heated at 90 °C for 3 d. A large quantity of colorless-plank crystals were obtained, which were washed with mother liquid, and dried under ambient conditions (yield: 73%, based on BIDPE). Anal. Calcd for C<sub>26</sub>H<sub>20</sub>O<sub>7</sub>N<sub>4</sub>Cd: C, 50.95, H, 3.29, N, 9.14; found C, 50.87, H, 3.31, N, 9.26. IR (KBr, cm<sup>−1</sup>): 3456(w), 3115(w), 1554(s), 1518(s), 1383(s), 1240(s), 1123(m), 1067(s), 1015(w), 964(w), 930(w), 855(m), 824(s), 745(s), 653(m), 531(m).

[*Co*(BIDPE)(5-OH-bdc)·H<sub>2</sub>O]<sub>*n*</sub> (**2**). Compound **2** was prepared by a procedure similar to that for the preparation of compound **1**, using Co(NO<sub>3</sub>)<sub>2</sub>·6H<sub>2</sub>O (29.1 mg, 0.1 mmol), 5-OH-H<sub>2</sub>bdc (18.2 mg, 0.1 mmol), and BIDPE (30.2 mg, 0.1 mmol) in 9 mL DMF/H<sub>2</sub>O (1:2, v/v). Purple crystals were obtained (yield: 66%, based on BIDPE). Anal.

Scheme 2. Crystallographically Established Coordination Modes of Carboxylic Groups in Compounds 1–6

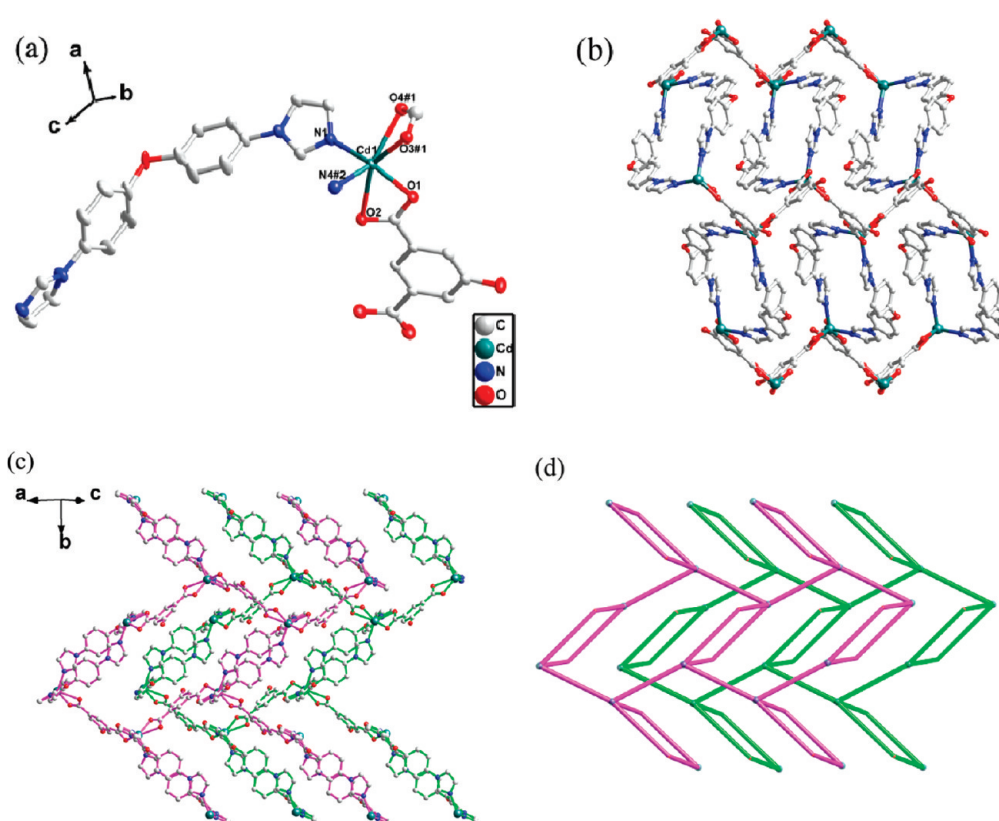
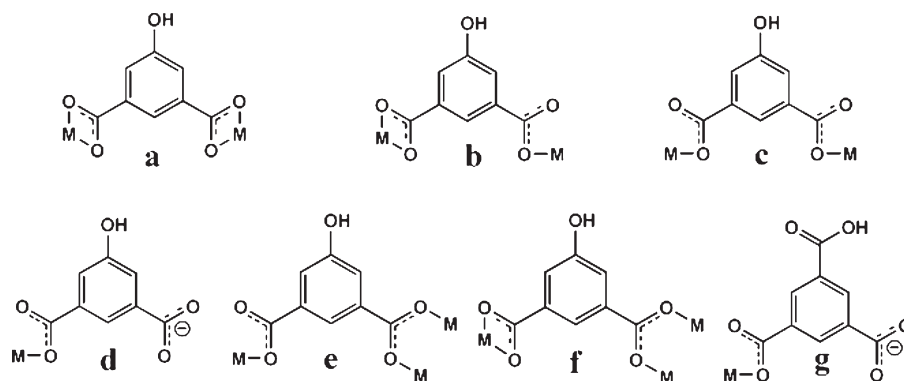


**Figure 1.** (a) Coordination environment of the Cd(II) ion in **1**. The hydrogen atoms are omitted for clarity. Symmetry codes: (#1)  $0.5 + x, 0.5 - y, -0.5 + z$ ; (#2)  $-x, -y, 2 - z$ . (b) Views of the 2D sheet by BIDPE ligands,  $5\text{-OH-bdc}^{2-}$  and Cd(II) ions. (c) Views of the 2D sheets with ABAB stack. (d) Schematic representation of 2D sheets of compound **1** with ABAB stack.

Calcd for  $\text{C}_{26}\text{H}_{20}\text{O}_7\text{N}_4\text{Co}$ : C, 55.82, H 3.60, N, 10.02; found C, 55.73, H, 3.71, N, 9.94. IR (KBr,  $\text{cm}^{-1}$ ): 3406(m), 3156(w), 2353(w), 1613(m), 1537(s), 1518(s), 1497(s), 1394(w), 1247(s), 1121(m), 1069(s), 966(w), 942(w), 839(m), 812(w), 772(s), 734(s), 656 (m), 526(m).

$[\text{Zn}_3(\text{BIDPE})_3(5\text{-OH-bdc})_3 \cdot 4\text{H}_2\text{O}]_n$  (**3**). Compound **3** was prepared by a procedure similar to that for the preparation of compound **1**, using  $\text{Zn}(\text{NO}_3)_2 \cdot 6\text{H}_2\text{O}$  (29.7 mg, 0.1 mmol),  $5\text{-OH-H}_2\text{bdc}$  (18.2 mg, 0.1 mmol) and BIDPE (28.4 mg, 0.1 mmol). A large quantity of colorless-plank crystals were obtained (yield: 53%, based on BIDPE). Calcd for  $\text{C}_{78}\text{H}_{62}\text{O}_{22}\text{N}_{12}\text{Zn}_3$ : C, 54.61, H 3.64, N, 9.80; found C, 54.48, H, 3.74, N 9.96. IR (KBr,  $\text{cm}^{-1}$ ): 3406(m), 3157(s), 1618(m), 1556(s), 1520(s), 1498(m), 1369(s), 1273(m), 1243(s), 1124(m), 1066(m), 966(m), 942(m), 836(w), 776(m), 567(m), 527(m).

$[\text{Ni}(\text{BIDPE})_2(5\text{-OH-bdc})(\text{H}_2\text{O}) \cdot 3\text{H}_2\text{O}]_n$  (**4**). A mixture of  $\text{Ni}(\text{NO}_3)_2 \cdot 6\text{H}_2\text{O}$  (29.1 mg, 0.1 mmol),  $5\text{-OH-H}_2\text{bdc}$  (18.2 mg, 0.1 mmol) and BIDPE (30.2 mg, 0.1 mmol) was added to 10 mL of  $\text{H}_2\text{O}$ , and the pH was adjusted to 7.0 via the addition of 1 M NaOH solution. The final mixture was placed in a Parr Teflon-lined stainless steel vessel (15 mL) under autogenous pressure and heated at  $130^\circ\text{C}$  for 2 d. Green crystals were obtained (yield: 66%, based on BIDPE). Anal. Calcd for  $\text{C}_{44}\text{H}_{40}\text{O}_{11}\text{N}_8\text{Ni}$ : C, 57.72, H 4.40, N, 12.24; found C, 57.64, H, 4.51, N, 12.30. IR (KBr,  $\text{cm}^{-1}$ ): 3261(w), 3095(w), 1609(m), 1563(s), 1514(s), 1390(m), 1344(s), 1265(m), 1237(s), 1167(m), 1122(m), 1066(s), 964(m), 936(m), 853(w), 834(m), 732(m), 711(m), 661(m), 534(m).

$[\text{Mn}_2(\text{BIDPE})_2(5\text{-OH-bdc})_2]_n$  (**5**). Compound **5** was prepared by a procedure similar to that for the preparation of compound **4**, using



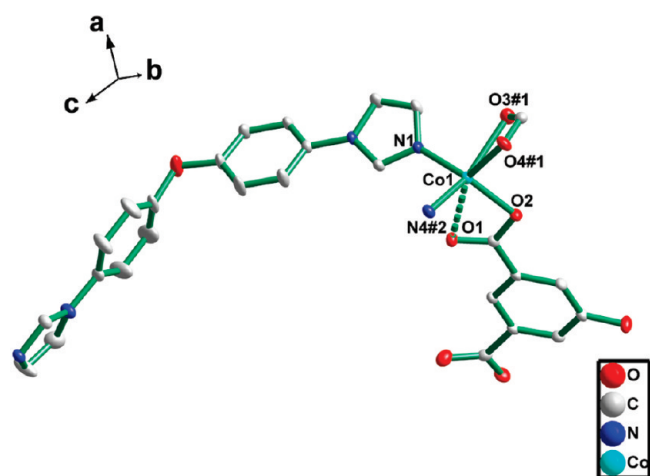


**Figure 2.** Coordination environment of the Co(II) ion in **2**. The hydrogen atoms are omitted for clarity. Symmetry codes: (#1)  $0.5 + x, 1.5 - y, -0.5 + z$ ; (#2)  $1 - x, 1 - y, 2 - z$ .

$\text{MnCl}_2 \cdot 4\text{H}_2\text{O}$  (19.8 mg, 0.1 mmol), 5-OH- $\text{H}_2\text{bdc}$  (18.2 mg, 0.1 mmol) and BIDPE (30.2 mg, 0.1 mmol) in 10 mL of  $\text{H}_2\text{O}$ , and the pH was adjust to 7.0 via the addition of 1 M NaOH solution. The final mixture was placed in a Parr Teflon-lined stainless steel vessel (15 mL) under autogenous pressure and heated at 110 °C for 2 d. A large quantity of pale yellow crystals were obtained (yield: ca. 46%, based on BIDPE). Anal. Calcd for  $\text{C}_{52}\text{H}_{36}\text{O}_{12}\text{N}_8\text{Mn}_2$ : C, 58.11, H 3.38, N, 10.43; found C, 58.19, H, 3.21, N, 10.40. IR (KBr,  $\text{cm}^{-1}$ ): 3248(w), 3136(w), 1617(m), 1549(s), 1513(s), 1420(m), 1378(s), 1266(s), 1241(s), 1167(m), 1122(m), 1066(s), 970(w), 926(w), 881(m), 820(m), 732(m), 711(m), 661(m), 534(m).

**[Ni(BIDPE)<sub>2</sub>(Hbtc)(H<sub>2</sub>O)]<sub>n</sub> (**6**).** A mixture of  $\text{Ni}(\text{NO}_3)_2 \cdot 6\text{H}_2\text{O}$  (29.7 mg, 0.1 mmol),  $\text{H}_3\text{btc}$  (10.5 mg, 0.05 mmol), and BIDPE (30.2 mg, 0.1 mmol) was added to 10 mL of  $\text{H}_2\text{O}$ , and the pH was adjusted to 6.0 via the addition of 1 M NaOH solution. The final mixture was placed in a Parr Teflon-lined stainless steel vessel (15 mL) under autogenous pressure and heated at 130 °C for 3 d. Green crystals were obtained (yield: 45%, based on BIDPE). Anal. Calcd for  $\text{C}_{45}\text{H}_{34}\text{O}_9\text{N}_8\text{Ni}$ : C, 60.76, H 3.85, N, 12.60; found C, 60.68, H, 3.77, N 12.71. IR (KBr,  $\text{cm}^{-1}$ ): 3134(w), 3075(w), 1685(s), 1634(s), 1602(w), 1553(s), 1512(s), 1448(m), 1375(s), 1268(s), 1240(s), 1128(w), 1103(m), 1064(m), 963(w), 938(w), 877(m), 836(w), 798(m), 760(s), 722(m), 663(m), 523(m).

**X-ray Crystallography.** Single crystals of **1–6** were prepared by the methods described in the synthetic procedure. X-ray crystallographic data of **1–6** were collected at room temperature using epoxy-coated crystals mounted on glass fiber. All measurements were made on a Bruker Apex Smart CCD diffractometer with graphite-monochromated Mo K $\alpha$  radiation ( $\lambda = 0.71073 \text{ \AA}$ ). The structures of complexes **1–6** were solved via direct methods, and the non-hydrogen atoms were located from the trial structure and then refined anisotropically with SHELXTL, using a full-matrix least-squares procedures based on  $F^2$  values.<sup>14</sup> The hydrogen atom positions were fixed geometrically at calculated distances and allowed to ride on the parent atoms. The distribution of peaks in the channels of **3** was chemically featureless to refine, using conventional discrete-atom models. To resolve these issues, the contribution of the electron density by the remaining solvent molecules were removed by the SQUEEZE routine in PLATON.<sup>15</sup> The numbers of solvent molecules in **3** were obtained by element analysis and thermogravimetric analysis. The relevant crystallographic data are presented in Table 1, while the selected bond lengths and angles are given in Table S1 in the Supporting Information.

## RESULTS AND DISCUSSION

**Crystal Structure of [Cd(BIDPE)(5-OH-bdc)·H<sub>2</sub>O]<sub>n</sub> (**1**).** X-ray analysis reveals that **1** crystallized in monoclinic space group  $P2_1/n$ . The asymmetric unit of **1** contains an independent Cd(II) cation, one 5-OH- $\text{bdc}^{2-}$  anion, one BIDPE ligand, and one lattice water molecule. As shown in Figure 1a, the Cd(II) center is 6-coordinated by four carboxylic O atoms from two 5-OH- $\text{H}_2\text{bdc}$  ligands and two nitrogen atoms from two BIDPE ligands to form a distorted octahedral geometry. The Cd–O lengths are in the range of 2.212(3)–2.587(3) Å and Cd–N lengths are 2.238(4)–2.253(4) Å, which are all similar to the values found in other Cd(II) complexes.<sup>16</sup>

Two BIDPE ligands connect two Cd(II) atoms to achieve a 32-membered  $[\text{Cd}_2(\text{BIDPE})_2]$  metallocyclic ring exhibiting maximum dimension of (corresponding to the Cd···Cd distance and O···O separation) 16.156 Å  $\times$  8.507 Å, and the N1–Cd–N4 angle is 96.01(15)°. Each completely deprotonated 5-OH- $\text{bdc}^{2-}$  anion coordinates to two Cd atoms by adopting chelating bidentate coordination modes (Scheme 2a). The extension of the structure into a 2D sheet is accomplished by 5-OH- $\text{bdc}^{2-}$  anions linking the  $[\text{Cd}_2(\text{BIDPE})_2]$  loops, as shown in Figure 1b. Each Cd atom is connected to three others via two 5-OH- $\text{bdc}^{2-}$  and two BIDPE ligands which all can be regarded as two connected linkers. In this analysis, the network topology features a 3-connected (6,3) net. As a result of the geometric characteristics of this two-dimensional (2D) sheet, the loops and the 2D layer are not in a plane, parts of BIDPE ligands can protrude into the cavities of the adjacent sheets, and the adjacent layers are stacked in an offset ABAB manner (Figure 1c and 1d).

**Crystal Structure of [Co(BIDPE)(5-OH-bdc)·H<sub>2</sub>O]<sub>n</sub> (**2**).** The coordination environment of **2** is a slightly different from that of **1**: Co(II) lies in a distorted trigonal bipyramidal coordination environment of three carboxylic O atoms from two 5-OH- $\text{bdc}^{2-}$  ligands and two nitrogen atoms from two BIDPE ligands (Figure 2). Carboxyl groups of 5-OH- $\text{bdc}^{2-}$  adopt two coordination modes: one carboxyl group adopts a monodentate coordination mode, whereas another carboxyl group coordinates to the same Co center by adopting a chelating coordination mode (Scheme 2b). Because the structure is very similar to that of compound **1**, we do not describe it any further.

**Crystal Structure of [Zn<sub>3</sub>(BIDPE)<sub>3</sub>(5-OH-bdc)<sub>3</sub>·4H<sub>2</sub>O]<sub>n</sub> (**3**).** X-ray analysis reveals that compound **3** is solved in orthorhombic space group  $Fdd2$ . The fundamental building unit of **3** contains three independent Zn(II) cations, three 5-OH- $\text{bdc}^{2-}$  anions, three BIDPE ligands, and four free water molecules. The 5-OH- $\text{bdc}^{2-}$  ions take the coordination modes 2b and 2c (Scheme 2). As shown in Figure 3a, Zn1(II) and Zn3(II) are 4-coordinated by two carboxylic O atoms from two 5-OH- $\text{H}_2\text{bdc}$  and two nitrogen atoms from two BIDPE ligands to form a distorted tetrahedral geometry, whereas the Zn2(II) is in an octahedral coordination environment of four carboxylic O atoms from two 5-OH- $\text{H}_2\text{bdc}$  and two nitrogen atoms from two BIDPE ligands. The Zn–O lengths are in the range of 1.968(4)–2.488(5) Å and the Zn–N lengths are 1.972(5)–2.048(6) Å, which are all similar to the values found in other Zn(II) complexes.<sup>17</sup>

5-OH- $\text{bdc}^{2-}$  anions link neighboring Zn(II) ions to form an infinitely 1D zigzag chain. The Zn···Zn distances are 9.556–9.938 Å. The BIDPE ligands link these zigzag chains to form a wavelike 2D sheet (Figure 3b). In this sheet, each 4-membered cycle is formed by four Zn(II) ions, two 5-OH- $\text{bdc}^{2-}$  anions, and two BIDPE ligands. The 2D sheet contains a larger channel (for the sake of clarity, the

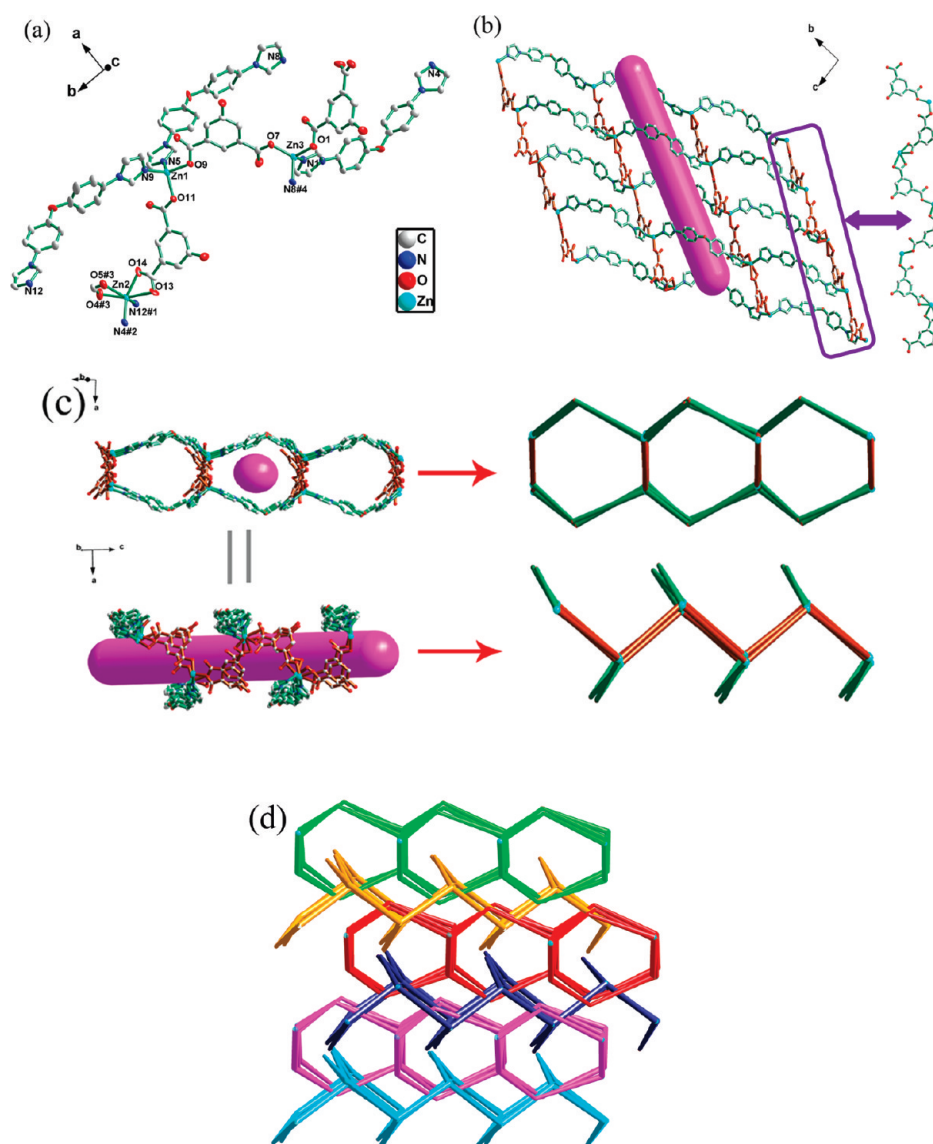


**Figure 3.** (a) Coordination environment of the Zn(II) ions in **3**. The hydrogen atoms are omitted for clarity. Symmetry codes: (#1)  $0.25 - x, -0.25 + y, -0.25 + z$ ; (#2)  $x, 1 + y, z$ ; (#3)  $0.25 - x, 0.75 + y, -0.25 + z$ ; (#4)  $0.25 - x, 0.25 + y, 0.25 + z$ . (b) Views of the wavelike 2D framework by 5-OH-bdc<sup>2-</sup>, BIDPE, and Zn ions along the *a*-axis. (c) Views of the reduced wavelike 2D framework in different directions. (d) Schematic representation of the 2D  $\rightarrow$  2D framework by six identical sheets.

purple rod was added), the size is  $\sim 15.633 \text{ \AA} \times 12.511 \text{ \AA}$ . The Zn(II) ions can be regarded as 4-connected nodes with all crystallographically independent 5-OH-bdc<sup>2-</sup> ligands acting as 2-connected linkers, and BIDPE ligands acting as V-shaped linkers. Therefore, the entire structure can be reduced as a (4,4) sheet (Figure 3c). The large channel within each sheet allows them to interpenetrate between the adjacent sheets in a “parallel interpenetration” fashion, resulting in a finite polycatenation. By analysis, only six of these identical sheets are polycatenated (Figure 3d).

To the best of our knowledge, among the known 2D interpenetrating polymers, most of the studies have focused on the 3-connected (6,3) or (4,4) networks, because of their large voids. The most examples are the mode of 2D  $\rightarrow$  2D interpenetration by adjacent nets or 2D  $\rightarrow$  3D polycatenation by infinite nets. However, finite identical networks ( $>3$ ) polycatenated were rarely reported, as evidenced in a review by Batten and Ciani.<sup>18</sup> As we know, this is the first report of six identical sheets polycatenated still to form a 2D  $\rightarrow$  2D network.

**Crystal Structure of  $[\text{Ni}(\text{BIDPE})_2(5\text{-OH-bdc})(\text{H}_2\text{O}) \cdot 3\text{H}_2\text{O}]_n$  (**4**).** The asymmetric unit of **4** contains one Ni(II) cation, one 5-OH-bdc<sup>2-</sup> anion, one BIDPE ligand, one coordinated water molecule, and three lattice water molecules. The 5-OH-H<sub>2</sub>bdc ligands take the coordination mode: one carboxyl group has monodentate coordination, and another is deprotonated as an anion (Scheme 2d). As shown in Figure 4a, each Ni(II) atom is six-coordinated by four N atoms from four BIDPE ligands, two O atoms from 5-OH-bdc<sup>2-</sup> anion and coordinated water molecule. The Ni–O lengths are 2.087(2)–2.102(2) Å and the Ni–N lengths are 2.082(3)–2.138(3) Å, which are similar to those found in other Ni(II) complexes.<sup>19</sup>

The neighboring Ni(II) ions are linked by BIDPE ligands and 5-OH-bdc<sup>2-</sup> anions to form infinitely double-stranded 1D chain. The adjacent distance of Ni  $\cdots$  Ni is 15.258 Å. Two BIDPE ligands connect two Ni(II) atoms to achieve a 32-membered  $[\text{Ni}_2(\text{BIDPE})_2]_n$  metallocyclic ring exhibiting maximum dimensions

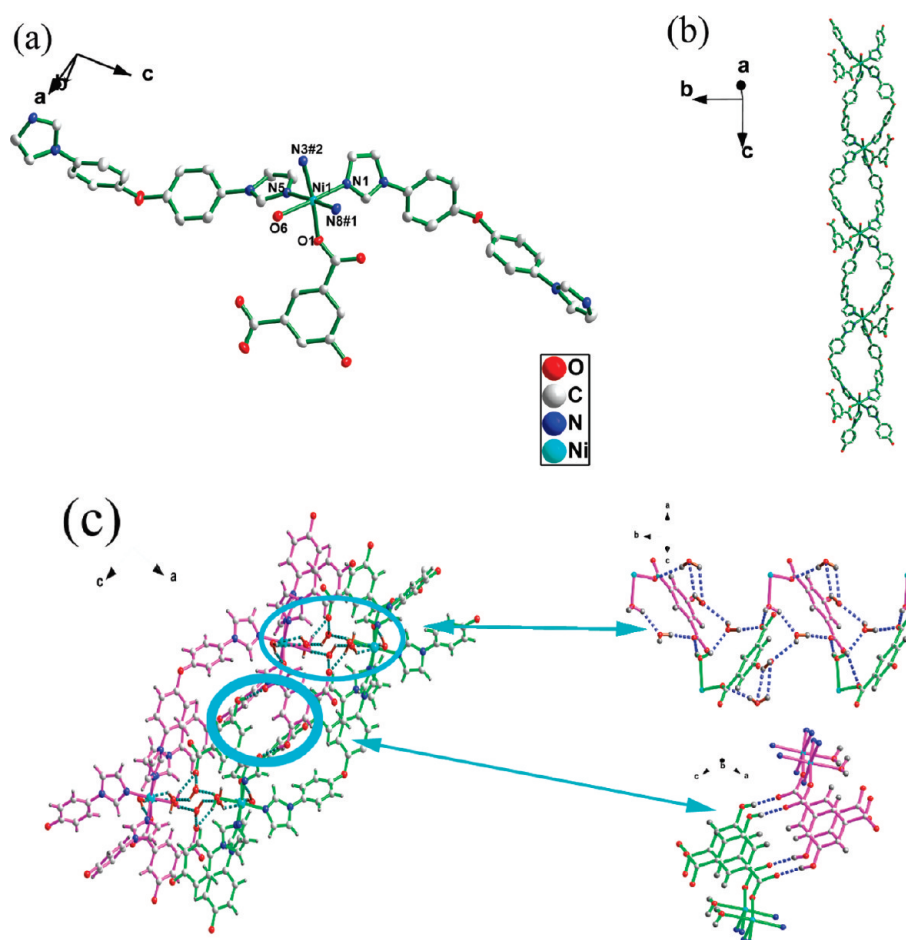


**Figure 4.** (a) Coordination environment of the Ni(II) ion in **4**. The hydrogen atoms are omitted for clarity. Symmetry codes: (#1)  $x, -y, 0.5 + z$ ; (#2)  $x, -y, -0.5 + z$ . (b) Views of the 1D double-stranded chain by 5-OH-bdc<sup>2-</sup> and Ni ions. (c) Views of the 3D network formed by hydrogen bondings.

of (corresponding to the Ni $\cdots$ Ni distance and O $\cdots$ O separation) 15.258 Å  $\times$  10.120 Å. The angles of N3–Ni–N5 and N1–Ni–N8 are 91.626(1)° and 93.389(1)°, respectively. In each 5-OH-bdc<sup>2-</sup> anion, only one carboxyl group coordinates to Ni atom, whereas another is deprotonated and acts as a counteranion (Figure 4b). Further inspection shows that the coordinated water, lattice water, carboxyl groups, and hydroxyl groups are actually contacting each other by strong hydrogen bonding (O $\cdots$ O distances range from 2.697 to 3.036 Å) (see Table S2 in the Supporting Information). These hydrogen bonds are composed of two parts: one contains coordinated water, lattice water, and carboxyl groups, whereas another is composed of hydroxyl groups and carboxyl groups (Figure 4c). Obviously, these hydrogen-bonded interactions are also available to increase the stability of the entire crystal structure of **4**. This extension of the structure into a three-dimensional (3D) framework is accomplished via hydrogen-bonded interactions.

**Crystal Structure of [Mn<sub>2</sub>(BIDPE)<sub>2</sub>(5-OH-bdc)<sub>2</sub>]<sub>n</sub> (**5**).** When Ni(NO<sub>3</sub>)<sub>2</sub> was replaced by MnCl<sub>2</sub>, a structurally different complex **5** was obtained. As shown in Figure 5a, **5** consists of two crystallographically independent Mn(II) ions, two BIDPE ligands, and two 5-OH-bdc<sup>2-</sup> anions. The 5-OH-bdc<sup>2-</sup> anions adopt three coordination modes. One carboxyl group adopts a bisonodentate coordination mode to bridge two Mn centers, one carboxylate group coordinates to the same Mn center by adopting a chelating coordination mode, and the other adopts

monodentate coordination mode (Scheme 2e and 2f). The Mn1(II) is in an octahedral coordination geometry coordinated by two nitrogen atoms from two BIDPE ligands (Mn1–N: 2.220(2)–2.229(2) Å) in the apical positions and four oxygen atoms from three 5-OH-bdc<sup>2-</sup> anions (Mn1–O: 2.108(2)–2.530(2) Å) in the equatorial positions. The Mn2(II) is five coordinated by two nitrogen atoms from two BIDPE ligands (Mn2–N: 2.225(2)–2.244(2) Å) and three oxygen atoms from three 5-OH-bdc<sup>2-</sup> anions (Mn2–O: 2.111(2)–2.149(2) Å).

In compound **5**, the Mn(II) atoms were bridged by carboxylate ligands to form a binuclear cluster with Mn $\cdots$ Mn separation of 4.922(3) Å. Each binuclear Mn was connected by four 5-OH-bdc<sup>2-</sup> anions to form a 1D ladder-shaped chain (Figure 5b). The BIDPE ligands share the binuclear Mn clusters with 5-OH-bdc<sup>2-</sup> anions to further generate an infinite 2D network (Figure 5c). In this network, each two BIDPE ligands linked two binuclear Mn clusters in a parallel fashion (Figure 5d). A better insight into the nature of this network can be achieved by the application of a topological approach. The binuclear Mn cluster can be regarded as 4-connected nodes with all crystallographically independent BIDPE ligands and 5-OH-bdc<sup>2-</sup> acting as 2-connected linkers. Therefore, the entire structure can be represented as a (4,4) sheet topology (Figure 5e).

**Crystal Structure of [Ni(BIDPE)<sub>2</sub>(Hbtc)(H<sub>2</sub>O)]<sub>n</sub> (**6**).** The crystal structure of **6** was solved in the space group  $P2_1/c$ . As depicted in Figure 6a, the structure contains one crystallographically



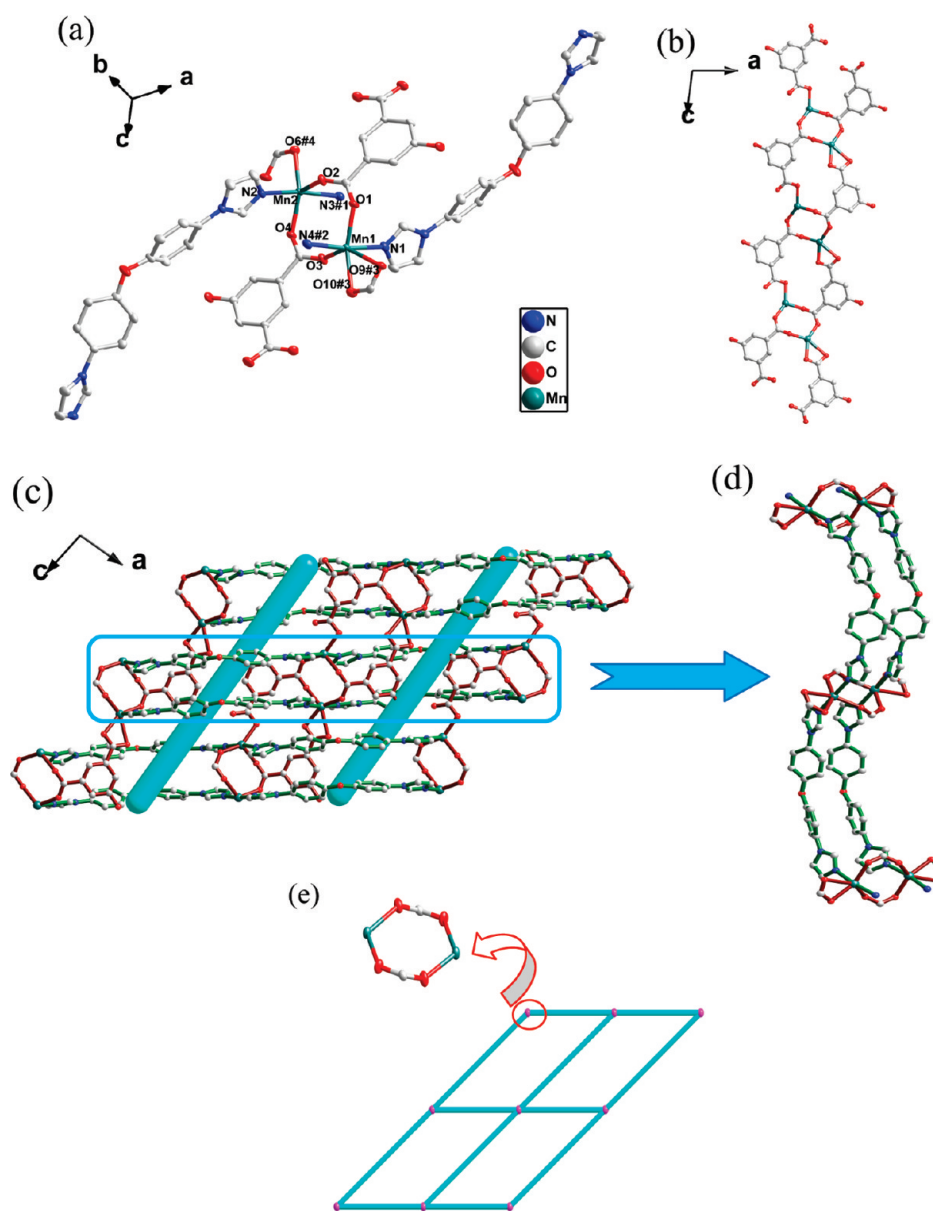


**Figure 5.** (a) Coordination environment of the Mn(II) ion in **1**. The hydrogen atoms are omitted for clarity. Symmetry codes: (#1)  $1 + x, 1.5 - y, -0.5 + z$ ; (#2)  $-1 + x, 1.5 - y, 0.5 + z$ ; (#3)  $x, 1.5 - y, 0.5 + z$ ; (#4)  $x, 1.5 - y, -0.5 + z$ . (b) Views of the 1D trapezoidal chain by  $\text{bdc}^{2-}$  and Mn ions along the  $b$ -axis. (c) Views of the 2D network. (d) Each two BIDPE ligands linked two binuclear Mn clusters in parallel fashion. (e) Schematic representation of the (4,4) sheet.

independent Ni(II) ion, two BIDPE ligands, one  $\text{Hbtc}^{2-}$  anion, and one coordinated water molecule. In **6**, the  $\text{H}_3\text{btc}$  displays an unusual mode of coordination, with only two carboxyl groups deprotonated: one carboxyl group coordinates to the Ni atom, and another acts as the counteranion (Scheme 2g). The Ni(II) ions has a disordered octahedral geometry with one carboxylic O atom from a  $\text{Hbtc}^{2-}$  anion, one coordinated water in the axial position, and four nitrogen atoms from four BIDPE ligands in the equatorial plane. The Ni–O lengths are 2.065(3)–2.148(2) Å and the Ni–N lengths are 2.091(2)–2.114(2) Å.

In compound **6**, each Ni atom is connected by BIDPE,  $\text{H}_3\text{btc}$ , and coordinated water to form a 2D puckered sheet. In the sheet, the four BIDPE ligands and four Ni atoms afford a square with a large window of  $16.221 \text{ Å} \times 16.067 \text{ Å}$ . The  $\text{Hbtc}^{2-}$  and water molecule share a Ni atom and fill in the grids (Figure 6b).

Because of the spacious nature of a single sheet, it allows another identical sheet to interlock with it, leading to a 2-fold interlocked structure (Figures 6c and 6e). These interlocked double sheets (red and green) are packed in an offset fashion. There are strong ( $\text{O} \cdots \text{H} \cdots \text{O}$ ) hydrogen bonds (the  $\text{O} \cdots \text{O}$  distance is 2.611 Å) between the interlocked sheets, which involve the coordinated water from one sheet and the carboxyl groups from another sheet, and vice versa. Similarly, these identical sheets (red or green) also exist as strong hydrogen bonds (the  $\text{O} \cdots \text{O}$  distance is 2.612 Å) formed by carboxyl groups among the sheets (see Table S3 in the Supporting Information). These hydrogen bonds change the framework from 2D to 3D (Figure 6d). Obviously, these hydrogen-bonded interactions increase the stability of the entire crystal structure of **6**, because it does not decompose until 390 °C. This suggests that carboxyl group and coordinated water

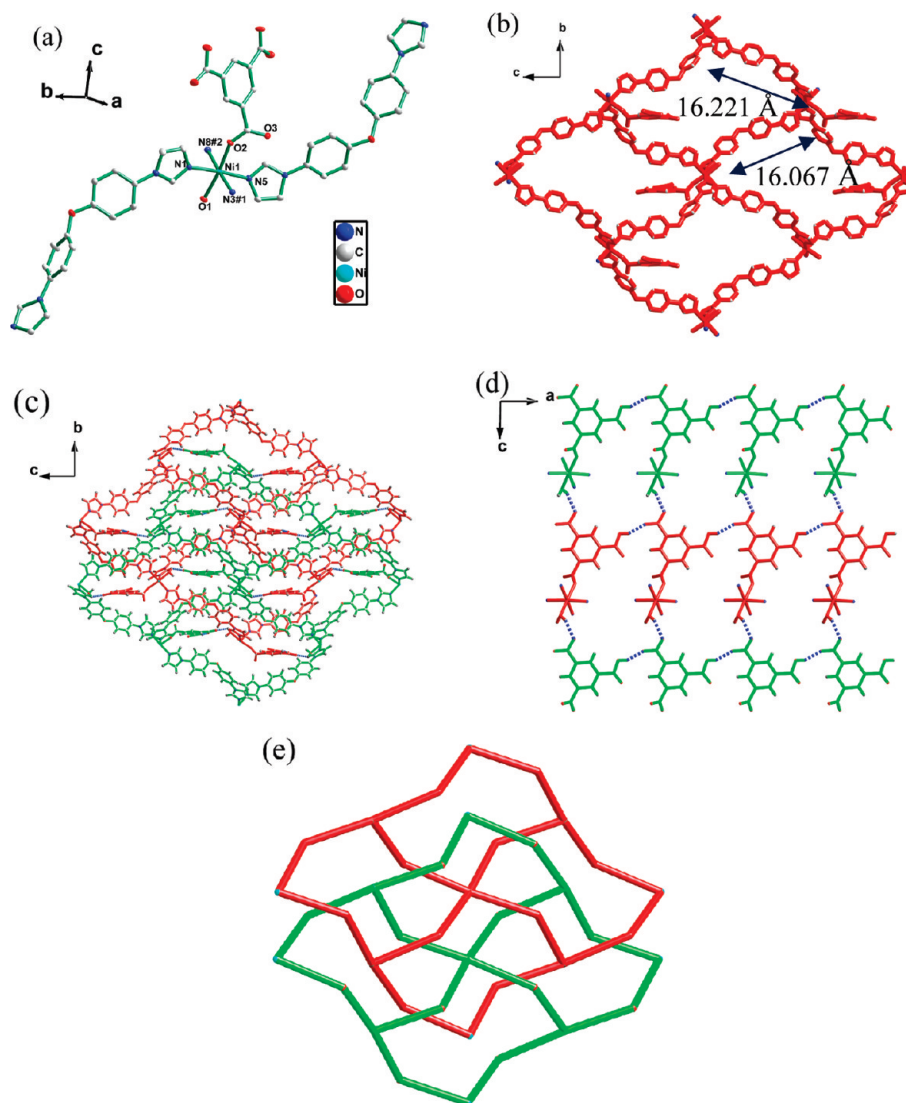


**Figure 6.** (a) Coordination environment of the Ni(II) ion in **6**. The hydrogen atoms are omitted for clarity. Symmetry codes: (#1)  $1 - x, -0.5 + y, -0.5 - z$ ; (#2)  $3 - x, 0.5 + y, 0.5 - z$ . (b) Views of the 2D puckered sheet along the *a*-axis. (c, d) Views of the 3D network formed by hydrogen bonds. (e) Schematic representation of the 2-fold interlocked sheets.

play an important role in increasing the dimension and sustaining the stabilization of the entire structure.

Compounds **1–6** have various structures; the results have shown that the different structures are evidently affected by the configuration of BIDPE. It can slightly adjust the angles to meet the requirement of coordination. The angles can be assessed by comparing the  $N \cdots O_{\text{core}} \cdots N$  angle defined by the central oxygen atom and the coordinated nitrogen atoms of the imidazole groups. To illuminate the influence of the angles, the angles are listed in Table 2. From these, we can know that BIDPE can adjust the corresponding angles from  $114.206^\circ$  to  $138.853^\circ$  to meet the requirement of coordination; when coordinated with 5-OH- $H_2$ bdc, the angles are smaller than that coordinated with  $H_3$ btc (the angle is up to  $138.853^\circ$ ). It is undoubtedly an ideal half-flexible N-containing ligand.

**Thermal Analysis and XRD Results.** To characterize the complexes more fully, in terms of thermal stability, their thermal behaviors were studied by TGA (see Figure S5 in the Supporting Information). For complex **1**, a rapid weight loss of 2.71% (calcd

**Table 2.** Different Angles of BIDPE Ligand

compound	angle ( $N \cdots O_{\text{core}} \cdots N$ )
<b>1</b>	$124.088^\circ$
<b>2</b>	$124.928^\circ$
<b>3</b>	$130.165^\circ, 128.619^\circ, 132.272^\circ$
<b>4</b>	$114.206^\circ, 115.522^\circ$
<b>5</b>	$128.191^\circ, 127.784^\circ$
<b>6</b>	$138.853^\circ, 132.810^\circ$

2.94%) is observed from  $50^\circ\text{C}$  to  $155^\circ\text{C}$ , which is attributed to the loss of the lattice water, and the structure was decomposes starting at  $388^\circ\text{C}$ . In the case of **2**, a weight loss is observed from  $20^\circ\text{C}$  to  $160^\circ\text{C}$ , which is attributed to the release of the lattice water with a weight loss of 3.04% (calcd 3.22%), and then the network collapses at  $400^\circ\text{C}$ . Compound **3** experienced a weight loss of 4.21% (calcd 4.12%) from  $20^\circ\text{C}$  to  $150^\circ\text{C}$ , which is attributed to the loss of four lattice water molecules, and the framework collapses at  $390^\circ\text{C}$ . For



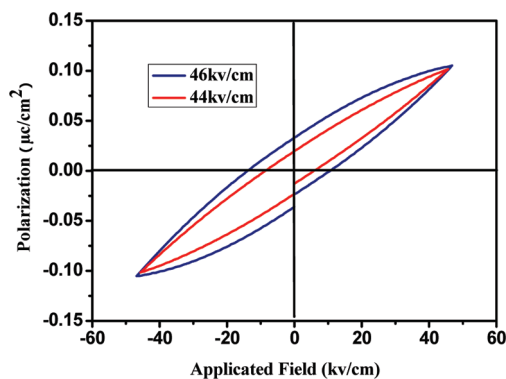


**Figure 7.** Polarization versus applied electric field curve (electric hysteresis loop of a powder pellet) of **3**.

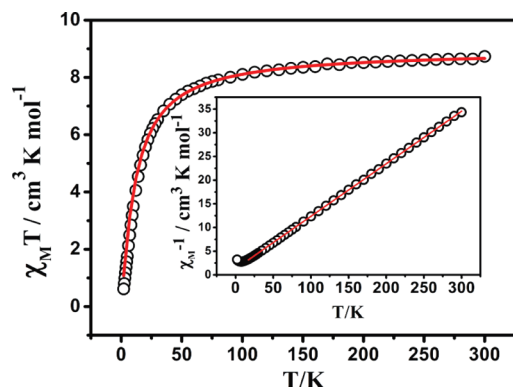


**Figure 8.** Temperature dependence of  $\chi_M T$  for **5** (inset: plot of  $\chi_M^{-1}$  versus  $T$ ; open circles represent experimental data, and the red line represents the fit of the data).

complex **4**, a rapid loss of one coordinated and three lattice water molecules was observed with a weight loss of 6.74% (calcd 6.73%) from 30 °C to 170 °C, and the structure decomposes at 340 °C. The anhydrous complex **5** begins to decompose at 420 °C. In the case of complex **6**, the network collapses at 390 °C. To confirm whether the crystal structures are truly representative of the bulk materials, powder XRD experiments were carried out for compounds **1–6**. The powder XRD experimental and computer-simulated patterns of the corresponding complexes in Figures S6–S11 in the Supporting Information show that the bulk synthesized materials and the measured single crystals are the same.

**Photochemical Properties.** Luminescent compounds are of great interest for their various applications in chemical sensors and photochemistry. The luminescent properties of free ligands BIDPE, 5-OH-H<sub>2</sub>bdc, and complexes **1** and **3** in the solid state at room temperature are investigated, as depicted in Figure S1 in the Supporting Information. Medium emissions of the free 5-OH-H<sub>2</sub>bdc and BIDPE ligands were observed at wavelengths of 350–410 nm ( $\lambda_{\text{max}} = 362$  and 395 nm), which could be attributed to the  $\pi^* \rightarrow \pi$  or  $\pi^* \rightarrow n$  transitions. Complexes **1** and **3** exhibit emission characteristics similar to the free ligands. The emission peaks at 417 nm ( $\lambda_{\text{ex}} = 365$  nm) in **1** and 415 nm ( $\lambda_{\text{ex}} = 362$  nm) in **3** show a small red shift, compared to that of the 5-OH-H<sub>2</sub>bdc and BIDPE ligands, which is probably due to the intraligand transition of the coordinated ligands. The enhancement of luminescence of complex **3** is mainly attributed to the polycatenated architecture, which causes a compact stack of

various atoms, enhancing the “rigidity” of the ligands and reducing the loss of energy by radiationless decay.<sup>20</sup> In addition, the UV–vis absorption spectra of compounds **1**, **2**, **3**, **4**, and **6** were carried out in the crystalline state at room temperature (BIDPE and 5-OH-H<sub>2</sub>bdc in solid state). As shown in Figure S2 in the Supporting Information, BIDPE and 5-OH-H<sub>2</sub>bdc show intense absorption peaks at 220–340 nm, which can be ascribed to  $\pi \rightarrow \pi^*$  transitions of the ligands. Energy bands of complex **2** from 500–600 nm, of complex **4** from 550–640 nm and 360–390 nm, and of complex **6** from 630–700 nm and 380–420 nm, are assigned as d–d transitions, while lower energy bands from 310–340 nm are probably assigned as metal-to-ligand charge-transfer (MLCT) transitions. These characteristic bands in this range do not appear in the spectra of the Cd<sup>2+</sup>, Zn<sup>2+</sup> complexes (see Figure S2 in the Supporting Information). A possible explanation for Cd<sup>2+</sup> and Zn<sup>2+</sup> could be found in their 3d<sup>10</sup> electronic states, which are more stable.<sup>21</sup> Furthermore, the emission decay lifetimes of compounds **1** and **3** were monitored and the curves are best fitted by biexponentials in the solid.<sup>22</sup> The emission decay lifetimes of the compounds **1** and **3** are as follows: complex **1**,  $\tau_1 = 4.455$  ns (19.85%) and  $\tau_2 = 1.132$  ns (80.15%) ( $\chi^2 = 1.072$ , see Figure S3 in the Supporting Information); complex **3**,  $\tau_1 = 1.729$  ns (28.68%) and  $\tau_2 = 3.991$  ns (71.32%) ( $\chi^2 = 1.196$ , see Figure S4 in the Supporting Information).

**Ferroelectric Property of Complex 3.** Complex **3** crystallizes in a noncentrosymmetric space groups (*fd*2), which is associated with the point groups of *C*<sub>2v</sub>, one of the 10 polar point groups (*C*<sub>1</sub>, *C*<sub>m</sub>, *C*<sub>2</sub>, *C*<sub>2v</sub>, *C*<sub>3</sub>, *C*<sub>3v</sub>, *C*<sub>4</sub>, *C*<sub>4v</sub>, *C*<sub>6</sub>, *C*<sub>6v</sub>) may have the potential to display ferroelectric behavior; thus, the ferroelectric feature was investigated. The electrical hysteresis loop of complex **3** was recorded at room temperature, using powdered samples in pellets.<sup>23</sup> Experimental results indicate the presence of electric hysteresis loops with a remnant electric polarization (*P*<sub>r</sub>) of 0.033 μC/cm<sup>2</sup> and an electric coercive field (*E*<sub>c</sub>) of 11.15 kV/cm; the spontaneous saturation polarization (*P*<sub>s</sub>) of complex **3** is ca. 0.105 μC/cm<sup>2</sup> (Figure 7), which is smaller than that of Zn powder sample [Zn(1,3-bibm)(D-ca)]<sub>n</sub> (*P*<sub>r</sub> = 0.052 μC/cm<sup>2</sup>, *P*<sub>s</sub> = 0.143 μC/cm<sup>2</sup>) and larger than [Zn(1,4-bibm)(D-ca)]<sub>n</sub> (*P*<sub>r</sub> = 0.022 μC/cm<sup>2</sup>, *P*<sub>s</sub> = 0.095 μC/cm<sup>2</sup>).<sup>24</sup> Respectively, they are all smaller than that of typical ferroelectric compound (e.g., NaKC<sub>4</sub>H<sub>4</sub>O<sub>6</sub>·4H<sub>2</sub>O (Rochelle salt), which usually has a saturation polarization of *P*<sub>s</sub> = 0.25 μC/cm<sup>2</sup>).

**Magnetic Properties of Complex 5.** The magnetic measurements were performed on polycrystalline samples of **5**, using a SQUID magnetometer under an applied field of 2000 Oe over a temperature range of 2–300 K. The temperature dependence of the magnetic susceptibility of **5** in the forms of  $\chi_M T$  and  $\chi_M$  versus  $T$  is displayed in Figure 5. At room temperature, the value of product  $\chi_M T$  is 8.73 cm<sup>3</sup> K mol<sup>−1</sup>, which agrees well with the expected value of 8.75 cm<sup>3</sup> K mol<sup>−1</sup> for two isolated high-spin Mn(II) ions ( $g = 2$  and  $S = 5/2$ ). Upon cooling, the  $\chi_M T$  value decreases continuously, reaching a value of 0.62 cm<sup>3</sup> K mol<sup>−1</sup> at 2 K, suggesting antiferromagnetic coupling.

The magnetic susceptibility data in the temperature range of 17–300 K can be well-fitted to the Curie–Weiss law with  $C = 9.02$  cm<sup>3</sup> mol<sup>−1</sup> K and  $\theta = -11.57$  K, which further confirms an overall antiferromagnetic interaction between the Mn<sup>II</sup> ions (Figure 8). Although this is observed at very low temperatures, where some anisotropy may be significant, Mn(II) is expected to

be Heisenberg-like in its magnetic behavior.<sup>25</sup> The best fit of the magnetic data above 2 K in terms of the Heisenberg 1-D chain, using eqs 1 and 2, and intrachain coupling  $J$  gives the following parameters:  $J = 0.62 \text{ cm}^{-1}$ ,  $zJ' = -0.92 \text{ cm}^{-1}$ , and  $g = 2.02$ . These results indicate that there exists very weak antiferromagnetic interaction within the  $\text{Mn}_2$  unit.<sup>26</sup>

$$\chi_M = \frac{2Ng^2\beta^2}{kT} \times \frac{55e^{30J/(kT)} + 30e^{20J/(kT)} + 14e^{12J/(kT)} + 5e^{6J/(kT)} + e^{2J/(kT)}}{11e^{30J/(kT)} + 9e^{20J/(kT)} + 7e^{12J/(kT)} + 5e^{6J/(kT)} + 3e^{2J/(kT)} + 1} \quad (1)$$

$$\chi_M = \frac{\chi}{1 - [2zJ'/(Ng^2\beta^2)]\chi} \quad (2)$$

## CONCLUSION

In summary, six new complexes (identified as **1–6**) have been synthesized via the self-assembly of BIDPE, 5-OH- $\text{H}_2\text{bdc}$ , and  $\text{H}_3\text{btc}$  ligands under solvothermal conditions. It was found that the BIDPE can change the angles to meet the requirements of coordination, and the carboxylic groups display a rich coordinated fashion. Complexes **1** and **2** have similar 2D frameworks. In the case of **3**, the noted feature is described as six identical 2D sheets that polycatenate to form a 2D  $\rightarrow$  2D framework. Complex **4** is an infinitely double-stranded 1D chain, which further generates a 3D framework via hydrogen-bonded interactions. Complex **5** contains binuclear Mn clusters. Complex **6** is a 2-fold interlocked 2D sheet with strong hydrogen bondings. The results demonstrate that the noncoordinated carboxyl groups of 5-OH- $\text{H}_2\text{bdc}$  and  $\text{H}_3\text{btc}$  can be well-used as the structure-directing tool and can produce various hydrogen bonding in the synthesis of unusual coordination frameworks. In addition, ferroelectric, magnetic, and photochemical properties have been studied. These properties reveal that they are potential multifunctional materials. Subsequent works will be focused on the structures and properties of a series of coordination complexes constructed by BIDPE with more auxiliary ligands and metal ions.

## ASSOCIATED CONTENT

**S Supporting Information.** Crystallographic data in CIF format, selected bond lengths and angles, and patterns of photochemistry, TGA, and powder XRD. This information is available free of charge via the Internet at <http://pubs.acs.org>.

## AUTHOR INFORMATION

### Corresponding Author

\*E-mails: zhenghg@nju.edu.cn (H. Z.), xue@ion.chem.utk.edu (Z. X.). Fax: 86-25-83314502.

## ACKNOWLEDGMENT

This work was supported by grants from the Natural Science Foundation of China (Nos. 91022011, 20971065, 21021062), National Basic Research Program of China (2007CB925103, 2010CB923303), and U.S. National Science Foundation (CHE-1012173 to Z.X.).

## REFERENCES

- (1) (a) Leininger, S.; Olenyuk, B.; Stang, P. J. *Chem. Rev.* **2000**, *100*, 853. (b) Rajput, L.; Vladimir, V.; Chernyshev; Biradha, K. *Chem. Commun.* **2010**, *35*, 6530. (c) Ma, Y.; Cheng, A. L.; Gao, E. Q. *Cryst. Growth Des.* **2010**, *7*, 2832. (d) Zou, R. Q.; Zhong, R. Q.; Du, M.; Kiyobayashia, T.; Xu, Q. *Chem. Commun.* **2007**, 2467.
- (2) (a) Pang, J.; Marcotte, E. J. P.; Seward, C.; Brown, R. S.; Wang, S. *Angew. Chem., Int. Ed.* **2001**, *40*, 4042. (b) Liang, K.; Zheng, H. G.; Song, Y. L.; Lappert, M. F.; Li, Y. Z.; Xin, X. Q.; Huang, Z. X.; Chen, J. T.; Lu, S. F. *Angew. Chem., Int. Ed.* **2004**, *43*, 5776. (c) Huang, Y. Q.; Ding, B.; Song, H. B.; Zhao, B.; Ren, P.; Cheng, P.; Wang, H. G.; Liao, D. Z.; Yan, S. P. *Chem. Commun.* **2006**, 4906. (d) Bauer, C. A.; Timofeeva, T. V.; Settersten, T. B.; Patterson, B. D.; Liu, V. H.; Simmons, B. A.; Allendorf, M. D. *J. Am. Chem. Soc.* **2007**, *129*, 7136. (e) Zheng, X. L.; Liu, Y.; Pan, M.; Lü, X. Q.; Zhang, J. Y.; Zhao, C. Y.; Tong, Y. X.; Su, C. Y. *Angew. Chem., Int. Ed.* **2007**, *46*, 7399. (f) Allendorf, M. D.; Bauer, C. A.; Bhakta, R. K.; Houka, R. J. T. *Chem. Soc. Rev.* **2009**, *38*, 1330. (g) Feng, R. F.; Jiang, L.; Chen, L.; Yan, C. F.; Wu, M. Y.; Hong, M. C. *Chem. Commun.* **2009**, 5296.
- (3) (a) Brechin, E. K.; Harris, S. G.; Harrison, A.; Parsons, S.; Whittaker, A. G.; Winpenny, R. E. P. *Chem. Commun.* **1997**, 653. (b) Lu, J. Y.; Lawandy, M. A.; Li, J. *Inorg. Chem.* **1999**, *38*, 2695. (c) Kumagai, H.; Kepert, C. J.; Kurmoo, M. *Inorg. Chem.* **2002**, *41*, 3410. (d) Cao, R.; Shi, Q.; Sun, D. F.; Hong, M. C.; Bi, W. H.; Zhao, Y. J. *Inorg. Chem.* **2002**, *41*, 6161. (e) Gavrilenko, K. S.; Punin, S. V.; Cadore, O.; Golhen, S.; Ouahab, L.; Pavlishchuk, V. V. *J. Am. Chem. Soc.* **2005**, *127*, 12246. (f) Pan, Z. R.; Zheng, H. G.; Wang, T. W.; Song, Y.; Li, Y. Z.; Guo, Z. J.; Batten, S. R. *Inorg. Chem.* **2008**, *47*, 9528. (g) Bi, Y. F.; Wang, X. T.; Wang, B. W.; Liao, W. P.; Wang, X. F.; Zhang, H. J.; Gao, S.; Lia, D. Q. *Dalton Trans.* **2009**, 2250.
- (4) (a) Wu, C. D.; Hu, A. G.; Zhang, L.; Lin, W. B. *J. Am. Chem. Soc.* **2005**, *127*, 8940. (b) Alaerts, L.; Seguin, E.; Poelman, H.; Starzyk, F. T.; Jacobs, P. A.; Vos, D. E. D. *Chem.—Eur. J.* **2006**, *12*, 7353. (c) Cho, S. H.; Ma, B.; Nguyen, S. T.; Hupp, J. T.; Albrecht-Schmitt, T. E. *Chem. Commun.* **2006**, 2563. (d) Xamena, F. X. L.; Abad, A.; Corma, A.; Garcia, H. J. *Catal.* **2007**, *250*, 294. (e) Liao, Z. L.; Li, G. D.; Bi, M. H.; Chen, J. S. *Inorg. Chem.* **2008**, *47*, 4844. (f) Wu, J.; Hou, H. W.; Guo, Y. X.; Fan, Y. T.; Wang, X. *Eur. J. Inorg. Chem.* **2009**, *19*, 2796. (g) Corma, A.; García, H.; Llabrés i Xamena, F. X. *Chem. Rev.* **2010**, *110*, 4606. (h) Malla Reddy, C.; Rama Krishna, G.; Soumyajit, G. *CrystEngComm* **2010**, *12*, 2296.
- (5) (a) Férey, G.; Latroche, M.; Serre, C.; Millange, F.; Loiseau, T.; Guégan, A. P. *Chem. Commun.* **2003**, 2976. (b) Rowsell, J. L. C.; Millward, A. R.; Park, K. S.; Yaghi, O. M. *J. Am. Chem. Soc.* **2004**, *126*, 5666. (c) Maji, T. K.; Mostafa, G.; Chang, H. C.; Kitagawa, S. *Chem. Commun.* **2005**, 2436. (d) Wong-Foy, A. G.; Matzger, A. J.; Yaghi, O. M. *J. Am. Chem. Soc.* **2006**, *128*, 3494. (e) Lin, X.; Jia, J.; Zhao, X.; Thomas, K. M.; Blake, A. J.; Walker, G. S.; Champness, N. R.; Hubberstey, P.; Schröder, M. *Angew. Chem., Int. Ed.* **2006**, *45*, 7358. (f) Liu, Y. L.; Eubank, J. F.; Cairns, A. J.; Eckert, J.; Kravtsov, V. C.; Luebke, R.; Eddaoudi, M. *Angew. Chem., Int. Ed.* **2007**, *46*, 3278. (g) Thallapally, P. K.; Tian, J.; Kishan, M. R.; Fernandez, C. A.; Dalgarno, S. J.; McGrail, P. B.; Warren, J. E.; Atwood, J. L. *J. Am. Chem. Soc.* **2008**, *130*, 16842. (h) Zhang, Y. B.; Zhang, W. X.; Feng, F. Y.; Zhang, J. P.; Chen, X. M. *Angew. Chem., Int. Ed.* **2009**, *48*, 5287. (i) Ma, L. Q.; Jin, A.; Xie, Z. G.; Lin, W. B. *Angew. Chem., Int. Ed.* **2009**, *48*, 9905. (j) Neofotistou, E.; Malliakas, C. D.; Trikalitis, P. N. *Chem.—Eur. J.* **2009**, *15*, 4523. (k) Lin, J. B.; Zhang, J. P.; Chen, X. M. *J. Am. Chem. Soc.* **2010**, *132*, 6654.
- (6) (a) Cui, Y.; Evans, O. R.; Ngo, H. L.; White, P. S.; Lin, W. B. *Angew. Chem., Int. Ed.* **2002**, *41*, 1159. (b) Yaghi, O. M.; O'Keeffe, M.; Ockwig, N. W.; Chae, H. K.; Eddaoudi, M.; Kim, J. *Nature* **2003**, *423*, 705. (c) Carballoa, R.; Covelloa, B.; López, E. M. V.; Martíneza, E. G.; Castiñeirasb, A.; Niclós, J. Z. *Anorg. Allg. Chem.* **2005**, *631*, 785. (d) Reger, D. L.; Watson, R. P.; Smith, M. D. *Inorg. Chem.* **2006**, *45*, 10077. (e) Luo, F.; Che, Y. X.; Zheng, J. M. *Cryst. Growth Des.* **2009**, *9*, 1066.
- (7) (a) Dybtsev, D. N.; Chun, H.; Kim, K. *Chem. Commun.* **2004**, 1594. (b) Dong, Y. B.; Xu, H. X.; Ma, J. P.; Huang, R. Q. *Inorg. Chem.* **2006**, *45*, 3325. (c) Tian, Y. Q.; Zhao, Y. M.; Chen, Z. X.; Zhang, G. N.

- Weng, L. H.; Zhao, D. Y. *Chem.—Eur. J.* **2007**, *13*, 4146. (d) Sarma, R.; Kalita, D.; Baruah, J. B. *Dalton Trans.* **2009**, 7428.
- (8) (a) Cao, R.; Sun, D. F.; Liang, Y. C.; Hong, M. C.; Tatsumi, K.; Shi, Q. *Inorg. Chem.* **2002**, *41*, 2087. (b) MacDonald, J. C.; Luo, T. J. M.; Palmore, G. T. R. *Cryst. Growth Des.* **2004**, *4*, 1203. (c) Mahata, P.; Natarajan, S. *Inorg. Chem.* **2007**, *46*, 1250. (d) Wang, Z. W.; Ji, C. C.; Li, J.; Guo, Z. J.; Li, Y. Z.; Zheng, H. G. *Cryst. Growth Des.* **2009**, *9*, 475.
- (9) (a) Masaoka, S.; Tanaka, D.; Nakanishi, Y.; Kitagawa, S. *Angew. Chem., Int. Ed.* **2004**, *43*, 2530. (b) Sun, D. F.; Ke, Y. X.; Mattox, T. M.; Ooro, B. A.; Zhou, H. C. *Chem. Commun.* **2005**, 5447. (c) Zheng, B.; Dong, H.; Bai, J. F.; Li, Y. Z.; Li, S. H.; Scheer, M. J. *Am. Chem. Soc.* **2008**, *130*, 7778. (d) Kanoo, P.; Gurunatha, K. L.; Maji, T. K. *Cryst. Growth Des.* **2009**, *9*, 4147.
- (10) (a) Qi, Y.; Che, Y. X.; Zheng, J. M. *CrystEngComm* **2008**, *10*, 1137. (b) Henninger, S. K.; Habib, H. A.; Janiak, C. *J. Am. Chem. Soc.* **2009**, *131*, 2776. (c) Ma, L. F.; Wang, L. Y.; Wang, Y. Y.; Du, Miao; Wang, J. G. *CrystEngComm* **2009**, *11*, 109. (d) Habib, H. A.; Sanchiz, J.; Janiak, C. *Inorg. Chim. Acta* **2009**, *362*, 2452. (e) Habib, H. A.; Hoffmann, A.; Hoppe, H. A.; Janiak, C. *Dalton Trans.* **2009**, 1742. (f) Habib, H. A.; Sanchiz, J.; Janiak, C. *Dalton Trans.* **2008**, 1734. (g) Zhang, L. P.; Yang, J.; Ma, J. F.; Jia, Z. F.; Xie, Y. P.; Wei, G. H. *CrystEngComm* **2008**, *10*, 1410. (h) Wisser, B.; Lu, Y.; Janiak, C. *Z. Anorg. Allg. Chem.* **2007**, *633*, 1189. (i) Manna, S. C.; Okamoto, K. I.; Zangrando, E.; Chaudhuri, N. R. *CrystEngComm* **2007**, *9*, 199. (j) Chen, Z. F.; Zhang, S. F.; Luo, H. S.; Abrahams, B. F.; Liang, H. *CrystEngComm* **2007**, *9*, 27. (k) Pichon, A.; Fierro, C. M.; Nieuwenhuyzen, M.; James, S. *CrystEngComm* **2007**, *9*, 449. (l) Pasan, J.; Sanchiz, J.; Lloret, F.; Julve, M.; Ruiz-Perez, C. *CrystEngComm* **2007**, *9*, 478. (m) Stephenson, M. D.; Hardie, M. J. *Dalton Trans.* **2006**, 3407. (n) Carballo, R.; Covelo, B.; Vazquez-Lopez, E. M.; García-Martínez, E.; Castiñeiras, A.; Janiak, C. *Z. Anorg. Allg. Chem.* **2005**, *631*, 2006. (o) Yao, J.; Lu, Z. D.; Li, Y. Z.; Lin, J. G.; Duan, X. Y.; Gao, S.; Meng, Q. J.; Lu, C. S. *CrystEngComm* **2008**, *10*, 1379. (p) Wei, G. H.; Yang, J.; Ma, J. F.; Liu, Y. Y.; Li, S. L.; Zhang, L. P. *Dalton Trans.* **2008**, 3080. (q) Zhang, J. Y.; Ma, Y.; Cheng, A. L.; Yue, Q.; Sun, Q.; Gao, E. Q. *Dalton Trans.* **2008**, 2061.
- (11) (b) Zaworotko, M. J. *Chem. Commun.* **2000**, 1. (a) Barnett, S. A.; Champness, N. R. *Coord. Chem. Rev.* **2003**, *246*, 145. (c) Roesky, H. W.; Andruh, M. *Coord. Chem. Rev.* **2003**, *236*, 91.
- (12) (a) Hoskins, B. F.; Robson, R.; Slizys, D. A. *Angew. Chem., Int. Ed.* **1997**, *36*, 2752. (b) Liu, H. K.; Sun, W. Y.; Ma, D. J.; Yu, K. B.; Tang, W. X. *Chem. Commun.* **2000**, 591. (c) Ma, J. F.; Yang, J.; Zheng, G. L.; Li, L.; Liu, J. F. *Inorg. Chem.* **2003**, *42*, 7531. (d) Zhao, W.; Fan, J.; Okamura, T.; Sun, W.-Y.; Ueyama, N. *New J. Chem.* **2004**, *28*, 1142. (e) Fan, J.; Hanson, B. E. *Inorg. Chem.* **2005**, *44*, 6998. (f) Cui, G. H.; Li, J. R.; Tian, J. L.; Bu, X. H.; Batten, S. R. *Cryst. Growth Des.* **2005**, *5*, 1775. (g) Wen, L. L.; Dang, D. B.; Duan, C. Y.; Li, Y. Z.; Tian, Z. F.; Meng, Q. J. *Inorg. Chem.* **2005**, *44*, 7161. (h) Yang, J.; Ma, J. F.; Liu, Y. Y.; Ma, J. C.; Batten, S. R. *Cryst. Growth Des.* **2008**, *8*, 4383. (i) Qi, Y.; Luo, F.; Che, Y. X.; Zheng, J. M. *Cryst. Growth Des.* **2008**, *8*, 606. (j) Li, F. F.; Ma, J. F.; Song, S. Y.; Yang, J.; Jia, H. Q.; Hu, N. H. *Cryst. Growth Des.* **2006**, *6*, 209. (k) Goodgame, D. M. L.; Menzer, S.; Williams, D. J. *Chem. Commun.* **1996**, 2127. (l) Hoskins, B. F.; Robson, R.; Slizys, D. A. *J. Am. Chem. Soc.* **1997**, *119*, 2952. (m) Carlucci, L.; Ciani, G.; Proserpio, D. M. *Chem. Commun.* **2004**, 380. (n) Wen, L. L.; Dang, D. B.; Duan, C. Y.; Li, Y. Z.; Tian, Z. F.; Meng, Q. J. *Inorg. Chem.* **2005**, *44*, 7161. (o) Zhu, H. F.; Fan, J.; Okamura, T.-a.; Sun, W. Y.; Ueyama, N. *Cryst. Growth Des.* **2005**, *5*, 289. (p) Lin, J.-D.; Li, Z.-H.; Li, J.-R.; Du, S.-W. *Polyhedron* **2007**, *26* (1), 107. (q) Song, L.; Li, J. R.; Lin, P.; Li, Z. H.; Li, T.; Du, S. W.; Wu, X. T. *Inorg. Chem.* **2006**, *45*, 10155. (r) Tian, Z. F.; Lin, J. G.; Su, Y.; Wen, L. L.; Liu, Y. M.; Zhu, H. Z.; Meng, Q. J. *Cryst. Growth Des.* **2007**, *7*, 1863. (s) Carlucci, L.; Ciani, G.; Maggini, S.; Proserpio, D. M. *Cryst. Growth Des.* **2008**, *8*, 162.
- (13) Hu, J. S.; Shang, Y. J.; Yao, X. Q.; Qin, L.; Li, Y. Z.; Guo, Z. J.; Zheng, H. G.; Xue, Z. L. *Cryst. Growth Des.* **2010**, *10*, 4135.
- (14) Bruker 2000, SMART (Version 5.0), SAINT-plus (Version 6), SHELXTL (Version 6.1), and SADABS (Version 2.03); Bruker AXS, Inc.: Madison, WI.
- (15) Van Der Sluis, P.; Spek, A. L. *Acta Crystallogr., Sect. A: Found Crystallogr.* **1990**, *46*, 194.
- (16) Dai, J. C.; Wu, X. T.; Fu, Z. Y.; Cui, C. P.; Hu, S. M.; Du, W. X.; Wu, L. M.; Zhang, H. H.; Sun, R. Q. *Inorg. Chem.* **2002**, *41*, 1391.
- (17) (a) Ma, L. F.; Wang, Y. Y.; Liu, J. Q.; Yang, G. P.; Du, M.; Wang, L. Y. *CrystEngComm* **2009**, *11*, 1800. (b) Thomas, A. Z.; Helmar, G.; Eckhard, D. *Polyhedron* **1998**, *17*, 2199.
- (18) Carlucci, L.; Ciani, G.; Proserpio, D. M. *Coord. Chem. Rev.* **2003**, *246*, 247.
- (19) Dong, Z.; Wang, Y. Yu.; Liu, R. T.; Liu, J. Q.; Cui, L.; Shi, Q. Z. *Cryst. Growth Des.* **2010**, *8*, 3311.
- (20) Yi, L.; Zhu, L. N.; Ding, B.; Cheng, P.; Liao, D. Z.; Yan, S. P.; Jiang, Z. H. *Inorg. Chem. Commun.* **2003**, *6*, 1209.
- (21) (a) Wang, B. C.; Wu, Q. R.; Hu, H. M.; Chen, X. L.; Yang, Z. H.; Shangguan, Y. Q.; Yang, M. L.; Xue, G. L. *CrystEngComm* **2010**, *12*, 485. (b) Jeremić, D. J.; Kaluderović, G. N.; Gómez-Ruiz, S.; Brčeski, I.; Kasalica, B.; Leovac, V. M. *Cryst. Growth Des.* **2010**, *10*, 559.
- (22) Li, X.; Sun, H. L.; Wu, X. S.; Qiu, X.; Du, M. *Inorg. Chem.* **2010**, *49*, 1865.
- (23) (a) Zhao, H.; Qu, Z. R.; Ye, Q.; Abrahams, B. F.; Wang, Y. P.; Liu, Z. G.; Xue, Z. L.; Xiong, R. G.; You, X. Z. *Chem. Mater.* **2003**, *15*, 4166. (b) Okubo, T.; Kawajiri, R.; Mitani, T.; Shimoda, T. *J. Am. Chem. Soc.* **2005**, *127*, 17598. (c) Ohkoshi, S. I.; Tokoro, H.; Matsuda, T.; Takahashi, H.; Irie, H.; Hashimoto, K. *Angew. Chem., Int. Ed.* **2007**, *46*, 3238. (d) Zhou, W. W.; Chen, J. T.; Xu, G.; Wang, M. S.; Zou, J. P.; Long, X. F.; Wang, G. J.; Guo, G. C.; Huang, J. S. *Chem. Commun.* **2008**, 2762. (e) Nakagawa, K.; Tokoro, H.; Ohkoshi, S. *Inorg. Chem.* **2008**, *47*, 10810. (f) Wang, C. F.; Li, D. P.; Chen, X.; Li, X. M.; Li, Y. Z.; Zuo, J. L.; You, X. Z. *Chem. Commun.* **2009**, 6940. (g) Zhao, H. R.; Li, D. P.; Ren, X. M.; Song, Y.; Jin, W. Q. *J. Am. Chem. Soc.* **2010**, *132*, 18.
- (24) Liang, X. Q.; Li, D. P.; Li, C. H.; Zhou, X. H.; Li, Y. Z.; Zuo, J. L.; You, X. Z. *Cryst. Growth Des.* **2010**, *6*, 2596.
- (25) Kennedy, B. J.; Murray, K. S. *Inorg. Chem.* **1985**, *24*, 1552.
- (26) (a) Chen, Z. L.; Jiang, C. F.; Yan, W. H.; Liang, F. P.; Batten, S. R. *Inorg. Chem.* **2009**, *48*, 4674. (b) Pan, Z. R.; Song, Y.; Jiao, Y.; Fang, Z. J.; Li, Y. Z.; Zheng, H. G. *Inorg. Chem.* **2008**, *47*, 5162.